developed, since the solutions of the equations of minimum surfaces can be represented in terms of analytic functions of a complex variable.

The author thanks A. F. Latypov for the advice given in the course of the investigation.

LITERATURE CITED

1. D. Gilbarg and M. Shiffman, "On bodies achieving extreme values of the critical Mach number. I," J. Rational Mech. Anal., 3, No. 2 (1954).
2. V. L. Berdichevskii, Variational Principles of Continuum Mechanics [in Russian], Nauka, Moscow (1983).
3. L. Bers, Mathematical Aspects of Subsonic and Transonic Gas Dynamics [Russian translation], IL, Moscow (1961).

NUMERICAL MODELING OF IMPULSIVE JETS OF A VISCOUS HEAT-CONDUCTING GAS

N. M. Bulgakova

UDC 533.6.001

Complete solution of the system of Navier–Stokes equations by the steady-state method with an implicit branching scheme for jets discharged from nozzles into a vacuum [1], submerged space [2], or companion flow [3] makes it possible to examine the subsonic sections of the flow and their effect on the structure of the jet as a whole. Additionally, the method proposed in [4, 5] makes it possible to calculate nonsteady processes. In the present study, we use this method to solve the problem of the discharge of a gas jet into a submerged space in the impulsive regime. This problem has application to both the formation of jets and the flow of quasisteady erosive jets.

1. Formulation of the Problem. We will examine a two-dimensional (axisymmetric) problem. Figure 1 presents a sketch of a region we are studying. It is bounded below by the axis of the jet OD. Line OA represents a sound outlet of radius r_e (or the edge of a supersonic nozzle). Above the edge of the nozzle, the boundary of the region of integration is a solid infinite 1 or finite 2 surface. As an alternative, AB may be a free boundary 3. The external boundary BC is located a distance from the axis such that the gas in the submerged space can be considered undisturbed. The boundary CD – where conditions corresponding to free discharge are established – is located a distance more than $20r_e$ from the nozzle edge.

The system of Navier–Stokes equations for a viscous compressible heat-conducting gas are written as follows in dimensionless form:

$$\frac{\partial \rho}{\partial t}+u\frac{\partial \rho}{\partial x}+v\frac{\partial \rho}{\partial y}+\rho\left(\frac{\partial u}{\partial x}+\frac{\partial v}{\partial y}+\frac{v}{y}\right)=0,$$

$$\frac{\partial u}{\partial t}+u\frac{\partial u}{\partial x}+v\frac{\partial u}{\partial y}+(\gamma-1)\frac{\partial e}{\partial x}+(\gamma-1)\frac{e}{\rho}\frac{\partial \rho}{\partial x}=$$

$$=\frac{1}{\mathrm{Re}\,\rho}\left\{\frac{4}{3}\frac{\partial}{\partial x}\mu\frac{\partial u}{\partial x}+\frac{\partial}{\partial y}\mu\frac{\partial u}{\partial y}+\frac{\mu}{y}\frac{\partial u}{\partial y}+\frac{\partial}{\partial y}\mu\frac{\partial v}{\partial x}-\right.$$

$$\left.-\frac{2}{3}\frac{\partial}{\partial x}\mu\frac{\partial v}{\partial y}+\frac{\mu}{y}\frac{\partial v}{\partial x}-\frac{2}{3}\frac{1}{y}\frac{\partial}{\partial x}(\mu v)\right\}, \qquad (1.1)$$

$$\frac{\partial v}{\partial t}+u\frac{\partial v}{\partial x}+v\frac{\partial v}{\partial y}+(\gamma-1)\frac{\partial e}{\partial y}+(\gamma-1)\frac{e}{\rho}\frac{\partial \rho}{\partial y}=$$

$$=\frac{1}{\mathrm{Re}\,\rho}\left\{\frac{\partial}{\partial x}\mu\frac{\partial v}{\partial x}+\frac{4}{3}\left(\frac{\partial}{\partial y}\mu\frac{\partial v}{\partial y}+\frac{\mu}{y}\frac{\partial v}{\partial y}+\frac{\mu v}{y^2}\right)+\frac{\partial}{\partial x}\mu\frac{\partial u}{\partial y}-\frac{2}{3}\frac{\partial}{\partial y}\mu\frac{\partial u}{\partial x}-\frac{2}{3}\frac{v}{y}\frac{\partial \mu}{\partial y}\right\},$$

$$\frac{\partial e}{\partial t}+u\frac{\partial e}{\partial x}+v\frac{\partial e}{\partial y}+(\gamma-1)e\left(\frac{\partial u}{\partial x}+\frac{\partial v}{\partial y}+\frac{v}{y}\right)=\frac{1}{\mathrm{Re}\,\rho}\left\{\frac{\gamma}{\mathrm{Pr}}\left(\frac{\partial}{\partial x}\mu\frac{\partial e}{\partial x}+\frac{\partial}{\partial y}\mu\frac{\partial e}{\partial y}+\frac{\mu}{y}\frac{\partial e}{\partial y}\right)+\right.$$

$$\left.+\frac{4}{3}\mu\left[\left(\frac{\partial u}{\partial x}\right)^2+\left(\frac{\partial v}{\partial y}\right)^2-\frac{\partial u}{\partial x}\frac{\partial v}{\partial y}\right]+\mu\left[\left(\frac{\partial u}{\partial y}\right)^2+\left(\frac{\partial v}{\partial x}\right)^2+2\frac{\partial u}{\partial y}\frac{\partial v}{\partial x}\right]+\frac{4}{3}\frac{\mu v}{y}\left(\frac{v}{y}-\frac{\partial v}{\partial y}-\frac{\partial u}{\partial x}\right)\right\}.$$

Novosibirsk. Translated from Prikladnaya Mekhanika i Tekhnicheskaya Fizika, No. 4, pp. 93-99, July-August, 1992. Original article submitted May 5, 1991; revision submitted July 5, 1991.

0021-8944/92/3304-0561$12.50

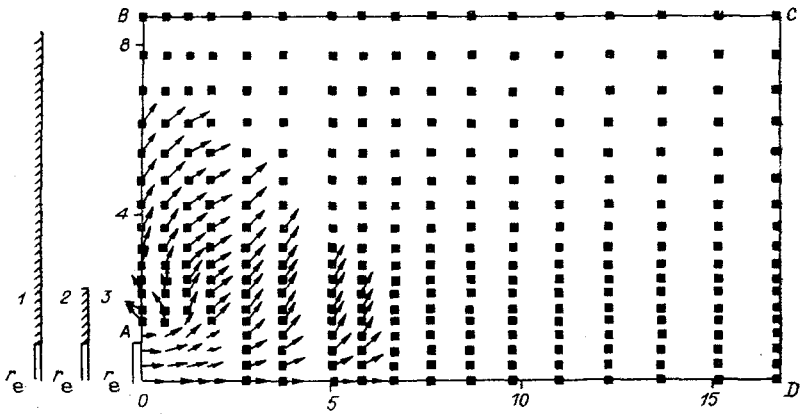

Fig. 1

Here, x, y is a rectangular coordinate system; t is time; u, v are components of the velocity vector along the axes x and y, respectively; γ is the adiabatic exponent; ρ is density; e is internal energy; Re, Pr are the Reynolds and Prandtl numbers.

We took the parameters on the edge of the nozzle r_e, ρ_e, u_e, e_e as the characteristic parameters. The system is supplemented by the equation of state $p = (\gamma - 1)\rho e$, so that $e_e = 1/(\gamma(\gamma - 1)M_e^2)$. Here, M_e is the Mach number on the nozzle edge. The temperature T was normalized relative to u_e^2. As in [2, 3], the temperature dependence of thermal conductivity λ and viscosity μ was assumed to conform to the Sutherland model [6]:

$$\frac{\lambda}{\lambda_e} = \frac{\mu}{\mu_e} = \left(\frac{T}{T_e}\right)^{3/2} \frac{T_e + T_s}{T + T_s}$$

(T_s is the Sutherland constant, assigned in relation to the species of outflowing gas).

As was noted above, when a jet is discharged into a submerged space, the boundary BC is removed from the OD axis a distance sufficient so that the external gas (flow) can be considered undisturbed. The following conditions of "free discharge" are used on the boundary CD and on AB above the solid wall or nozzle edge (in the absence of a wall):

$$\partial f/\partial x = 0 \quad \text{or} \quad \partial^2 f/\partial x^2 = 0 \quad (f = (\rho, u, v, e)). \tag{1.2}$$

The same condition is imposed on the boundary BC in the case of discharge of the jet into a vacuum [1].

The parameters are assumed to be constant and equal to $f_e = (\rho_e, u_e, 0, e_e)$ on the nozzle edge. We either assume that adsorption takes place on the edge $u_e(0, 1) = 0$ or we assign a parabolic profile. The flow is symmetric relative to the jet axis OD:

$$\partial\rho/\partial y = \partial u/\partial y = v = \partial e/\partial y = 0.$$

We use flow adsorption conditions on the solid surface:

$$u(0, y) = v(0, y) = 0,\ T(0, y) = T_w = \text{const},\ \partial p/\partial x|_{x=0} = 0 \tag{1.3}$$

or slip conditions (written in dimensionless variables):

$$u(0, y) = 0,\ \left.\frac{\partial p}{\partial x}\right|_{x=0} = 0,$$
$$v(0, y) = \frac{2-\sigma}{\sigma}\,\mathrm{Kn}\left.\frac{\partial v}{\partial x}\right|_{x=0} + \frac{3}{4}\frac{\mu}{\rho T\,\mathrm{Re}}\left.\frac{\partial T}{\partial y}\right|_{x=0},\quad T(0, y) = T_w + \frac{2-\alpha}{\alpha}\frac{2\gamma}{\gamma-1}\,\mathrm{Kn}\left.\frac{\partial T}{\partial x}\right|_{x=0}. \tag{1.4}$$

Here, Kn is the Knudsen number, determined on the basis of the radius of the nozzle; T_W is the temperature of the wall; σ is the fraction of diffusely reflected molecules; α is the accomodation coefficient (we took $\sigma = \alpha = 1$).

To obtain a stationary parameter distribution, we assigned the initial conditions as follows. In the cylindrical region of radius r_e next to the axis, we assigned parameters equal to the parameters on the nozzle edge. In the rest of the region, the assigned values were equal to those in the undisturbed gas. In the case of the solution of the nonsteady problem, we assigned initial conditions analogous to the instantaneous rupture of a membrane at the edge of the nozzle. Thus, the gas in the submerged space could be considered undisturbed at the initial moment of time.

The theoretical region contained [$N_x \times N_y$] points (N_x = 40-50, N_y = 30-60) and was subdivided by a nonuniform grid in relation to the degree of underexpansion. Here, we took one of two approaches: we increased the density of the grid toward the edge of the nozzle in accordance with a logarithmic law; we used an arithmetic progression to decrease the density of the grid with increasing distance from the nozzle edge. The grid was used to construct a difference scheme that involved branching with respect to the coordinates and physical processes [4, 5]. The scheme is stable at Curant numbers $K \leqslant 10$: $K = \frac{\tau}{h_x h_y}(h_x|v| + h_y|u| + c\max(h_x, h_y))$ (h_x and h_y are the mesh sizes of the grid along the x and y axes; c is sonic velocity).

The scheme was written in Cartesian coordinates on the basis of the principle described in [5]. It has four fractional steps at each time step, with a different matrix operator Ω_i (i = 1, 2, 3, 4) being introduced at each fractional step. The operators Ω_1 and Ω_2 account for convective heat transfer and the viscous terms (without mixed derivatives) along the x and y axes, respectively. The matrix operators Ω_3 and Ω_4 contain the terms with pressure and terms of the type div v. The remaining terms are introduced at the first fractional step. The convective terms are approximated by first-order differences with allowance for the sign of velocity, while the remaining terms are approximated by first- or second-order differences. We introduce matrix operators Ω_i (i = 1, 2, 3, 4) in the first fractional step to write the right sides of the equations, these operators differing from Ω_i in that all of the derivatives written in Ω_i are of the second order (first derivative with allowance for the sign of velocity on a three-point scale). The system is realized by means of scalar trial runs at each fractional step. The section approximates the initial system of equations (1.1) with first- (in the nonsteady case) or second-order (in the steady case) accuracy [5].

The iteration parameter τ in the calculations was varied from 0.01 to 0.2. With a change in τ by one order, the maximum deviation among the distributions of ρ, u, v, and e obtained at identical moments of time was no greater than 1.5%. As was shown by the calculations, the optimum value of the iteration parameter τ = 0.1.

The calculations were performed with the following parameters: $1 \leqslant M_e \leqslant 6$, $20 \leqslant Re \leqslant 10^5$, $0.5 \leqslant n \leqslant 10^3$ ($n = p_e/p_\infty$ is the degree of underexpansion). The adiabatic exponent γ was taken equal to 1.4 and 1.67, Pr = 0.72.

2. Examples of Numerical Calculations. To check the accuracy of the program, we performed calculations for a steady jet discharged into a submerged space. The calculations were performed for the variants M_e = 1, Re = 10^3, n = 10, T_e/T_∞ = 1 and M_e = 1, Re = 112, n = 18.5, T_e/T_∞ = 1 using the formulation in [2]. Agreement was obtained with the results in [2].

Pressure Pulsations in the Interaction of Laser Radiation with a Flat Target. With the startup of the jet, significant pressure pulsations develop on solid surfaces adjacent to the nozzle. This problem is important in aerospace engineering [7]. Significant pressure pulsations were observed on the target in experiments in [8] involving the interaction of laser radiation with a substance. In this case, the radius of the radiation was smaller than the radius of the target. Several hypotheses have been advanced in regard to the nature of the pulsations. For example, it has been proposed that the pulsations occur in an oscillatory regime in which the radiation is screened by erosion products [9]. However, this hypothesis does not explain many of the effects that have been observed experimentally. Kuznetsov [8] suggested that the pulsations are of a gas-dynamic nature.

We will examine an erosive flame as a sonic jet. Ionization processes undoubtedly affect the gasdynamic structure of the jet, changing the position of characteristic shock waves [10]. However, the gasdynamic pattern of the jet and an erosive flame remain qualitatively similar. It is assumed that the jet is formed instantaneously. Before the moment of formation, the force (total pressure) acting on the target is equal to zero. At the initial moment of time, pressure is equal to the reactive force of the jet. Then the gas of the submerged space is brought into motion. It was assumed that the gas on the back side of the target was stationary. Figure 2 shows the time dependence of total pressure on the target $\hat{p} = \int_s p\,ds$ (the lateral surfaces of the target were not considered, i.e., the target was assumed to be infinitely thin). Here, the quantity $\hat{p}$ was normalized for pressure on the edge p_e and the area of the radiation spot. The solid line shows theoretical data for the case n = 1.1, with a target radius $r_t = 2r_e$ (where r_e is the radius of the radiation spot) and a ratio of target-surface temperature to the temperature of the gas in the submerged space

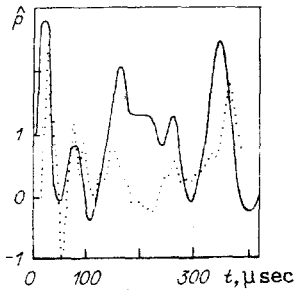

Fig. 2

$T_e/T_\infty = 2$, $Re = 10^3$. The points represented the empirical curve of total pressure $\hat{p}$ from [8]. The figure shows previously unpublished data obtained from the irradiation of the surface of a magnesium target by a laser pulse. Here, the radius of the target was twice as great as the radius of the radiation spot, and the empirically measured degree of underexpansion n = 1.1. It is evident from the graph that the amplitude of the pulsations is similar in the calculations and the experiment and that a negative $\hat{p}$ is obtained. This result cannot be explained from the viewpoint of the theory proposed in [9]. Uglov and Selishchev [9] also obtained almost harmonic pressure oscillations, but the pulsations obtained in both the calculation and the experiment were irregular. Thus, combination of the theoretical and experimental data provides support for the pulsation mechanism proposed in [8].

Calculations performed for sonic jets with different values of n permit the conclusion that, for jets with n = 1-50, an increase in n is accompanied by shortening of the transient period. The decay in pulsations seen experimentally with an increase in n means that the jet flow reaches the steady state. Thus, at n = 50, the calculated time until establishment of the steady-state regime is about 300 μsec. This is about half the life of the erosive flame in [8]. At n = 2, the period before the steady state is reached is considerably greater than the life of the erosive flame. The pattern of initiation of sonic and supersonic jets is of independent interest.

Initiation of Jets. In a two-dimensional formulation, the problem of the initiation of a jet is properly solved within the framework of the complete system of Navier–Stokes equations. This is because the motion which takes place involves the gas of a submerged space and the formation of vortical flows with a subsonic velocity. The vortices may have an effect on the structure of the entire flow. The initiation and development of a vortex structure was observed in experiments in [11] during the formation of sonic and supersonic jets.

We performed a series of calculations on the formation of jets with different degrees of underexpansion. In the presence of an infinite surface adjacent to the nozzle (boundary conditions 1 in Fig. 1), a vortex is formed near the nozzle in the submerged state. This vortex serves to bring gas closer to the wall, the same gas then being drawn away from the wall by the jet due to viscosity. Such a vortex structure also figured in the calculations performed in [2, 12].

Figure 3 shows the development of the sonic jet obtained in the calculations in the present study for the case of the absence of a solid surface adjacent to the nozzle (boundary conditions 3 in Fig. 1) for n = 2, $T_e/T_\infty = 2$, $Re = 10^3$. The figure shows the flow fields at different moments of time after formation of the jet. The number of iterations is shown in the top right corner. This number can be converted to real time for an actual nozzle size. For the conditions in the experiments in [8], these values would be 158, 237, and 632 μsec. For the same case, Fig. 1 shows the pattern corresponding to the formation of the jet at 25 iterations – which corresponds to 20 μsec.

It should be noted that all of the vectors in the graphical system we used were normalized for maximum velocity. In this case, if the velocity vector is roughly 15% of the maximum velocity for the given case, the vector is depicted in the standard manner with an established length and its base is enclosed in a square. Vectors close to the maximum are drawn without a square in the base [13]. This makes it possible to readily differentiate even weak gas flows. It is evident from Fig. 3 that a vortical flow is generated near the nozzle edge, this flow being entrained downstream in the process of establishment of the jet. More developed vortical flows are formed in the presence of a small surface adjacent to the nozzle. In this case, several vortices that move downstream in succession may be formed. It is also

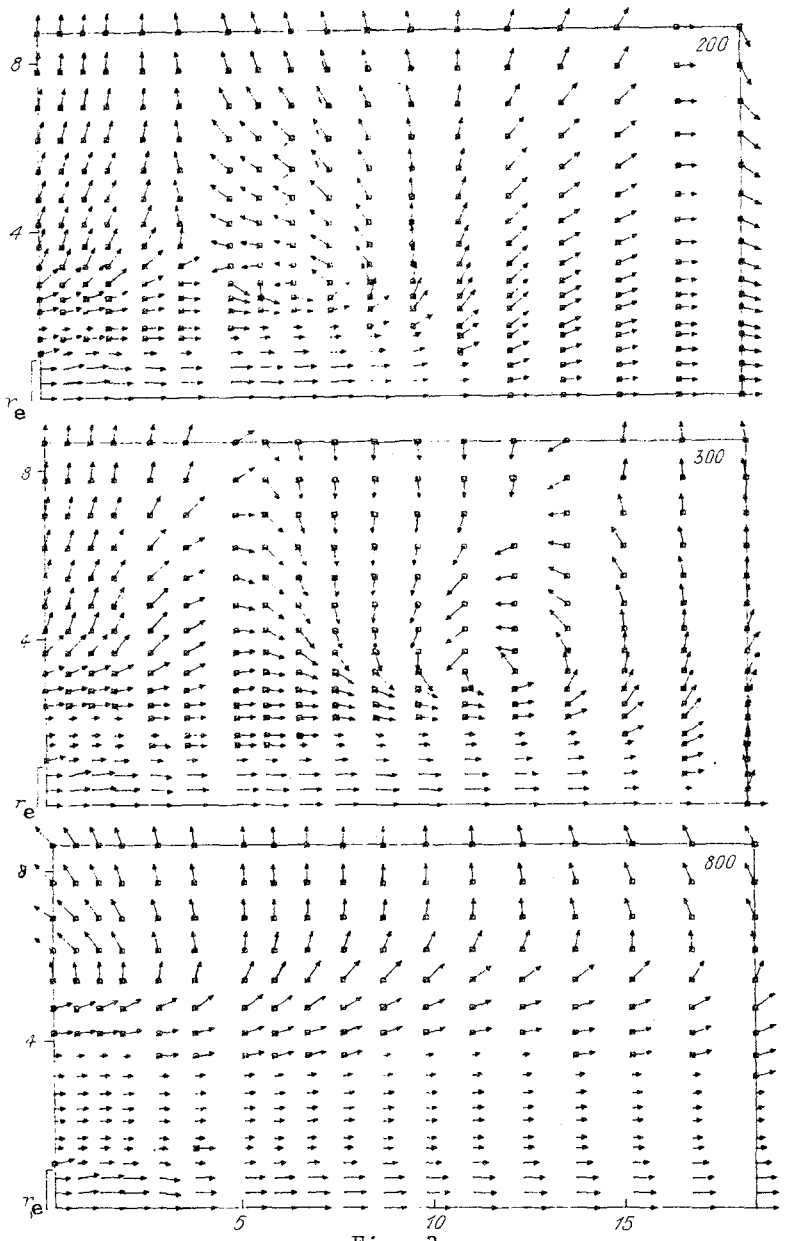

Fig. 3

evident from Fig. 3 that well-developed ejection is established as the jet is formed. If even a small surface is adjacent to the nozzle, the ejection process is weakened greatly.

There are also a number of interesting flows that are formed with the initiation of jets both on the ground and in space [14]. For example, a reverse flow is formed in the frontal part of a jet penetrating a submerged space. Smorr et al. [14] termed such flows cocoons and performed calculations for them for n = 1. Beginning at M = 2 or more, a cocoon was formed in [14] with the discharge of a low-density jet into a denser gas. Here, the calculations were performed within the framework of two-dimensional Eulerian hydrodynamics. We also used the complete system of Navier–Stokes equations to obtain a reverse flow with the formation of vortices in the front part of a jet that had a structure similar to the structure in [14].

Figure 4 shows the flow field corresponding to the discharge of a gas with n = 2 from a sonic nozzle into the gas of a submerged space with the same mass and a temperature twice as great as the temperature in the outlet section of the nozzle $T_e/T_\infty = 1/3$, $Re = 10^3$ (compare with Fig. 13 in [14]). Thus, flow reversal occurs both with the discharge of a jet of rarefied gas into a dense gas and with the discharge of a jet of cold gas into a hot gas. The subsequent development of the process involves the onset of turbulent mixing due to the development of vortical flows.

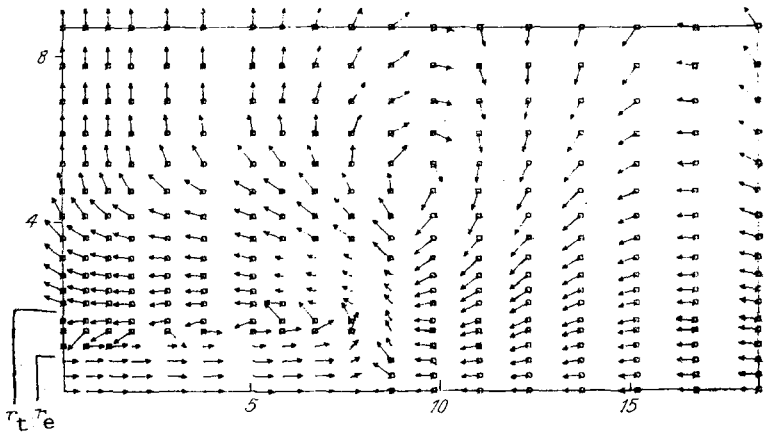

Fig. 4

The case shown in Fig. 4 corresponds to a sonic jet. Thus, with a high degree of underexpansion, the formation of a cocoon occurs at lower Mach numbers than in [4] due to expansion of the jet in the submerged space.

In conclusion, we note that the solution of a steady-state problem with the above initial conditions requires 40-50 min on a BÉSM-6 computer (250-300 iterations). The solution of nonsteady problems depends on the initial and boundary conditions and, for various problems, takes from 40 min to several hours on a BÉSM-6.

The author thanks L. I. Kuznetsova for commenting on the study and providing empirical data.

LITERATURE CITED

1. A. V. Beloshitskii and E. N. Bondarev, "Discharge of a viscous gas from a cylindrical channel into a vacuum," Izv. Akad. Nauk SSSR, Mekh. Zhidk. Gaza, No. 1 (1981).
2. B. D. Kovalev and V. I. Myshenkov, "Calculation of a viscous supersonic jet being discharged into a submerged space," Uch. Zap. TsAGI, 9, No. 2 (1978).
3. B. D. Kovalev and V. I. Myshenkov, "Calculation of a viscous supersonic jet being discharged into a companion flow," ibid., 9, No. 3 (1978).
4. Yu. A. Berezin, V. M. Kovenya, and N. N. Yanenko, "Implicit scheme to calculate the flow of a viscous heat-conducting gas," ChMMSS, 3, No. 4 (1972).
5. Yu. A. Berezin, V. M. Kovenya, and N. N. Yanenko, "Difference method of solving problems involving flow about bodies in "natural" coordinates," in: Aeromechanics [in Russian], Nauka, Moscow (1976).
6. J. Hierschfelder, J. Curtis, and R. Beard, Molecular Theory of Gases and Liquids, Wiley-Interscience, New York (1964).
7. M. C. Cline and R. G. Wilmoth, "Computation of the space shuttle solid rocket booster nozzle start-up transient flow," AIAA Pap., No. 0462 (1984).
8. L. I. Kuznetsov, "Pressure oscillations on a target subjected to pulsed laser radiation," Zh. Tekh. Fiz., 60, No. 8 (1990).
9. A. A. Uglov and S. V. Selishchev, Oscillatory Processes in the Action of Concentrated Energy FLows [in Russian], Nauka, Moscow (1978).
10. N. M. Bulgakova, "Disposal of a plasmoid into the atmosphere," in: Nonequilibrium Processes in One- and Two-Phase Systems [in Russian], IT SO AN SSSR, Novosibirsk (1981).
11. V. A. Belavin, V. V. Golub, and I. M. Naboko, "Structure of impulsive gas jets discharged from supersonic nozzles," Prikl. Mekh. Tekh. Fiz., No. 1 (1979).
12. R. Walther and J. Algermissen, "Numerische Integration der instationaren Strömungsgleichungen am Beispiel eines ebenen Überschallfreistrahls," Forsch. Ingenieurwes., 49, No. 3 (1983).
13. Methodological Recommendations of the Use of the SIGAM Graphical System, SNIIGGiMS, Novosibirsk (1988).
14. L. L. Smorr, M. L. Norman, and A. K.-H. Winkler, "Shocks, interfaces, and patterns in supersonic jets," Physica D, 12, No. 1 (1984).